



HAL
open science

Nascent DNA Proteomics Reveals a Chromatin Remodeler Required for Topoisomerase I Loading at Replication Forks

Cyril Ribeyre, Ralph Zellweger, Maëva Chauvin, Nicole Bec, Christian Larroque, Massimo Lopes, Angelos Constantinou

► **To cite this version:**

Cyril Ribeyre, Ralph Zellweger, Maëva Chauvin, Nicole Bec, Christian Larroque, et al.. Nascent DNA Proteomics Reveals a Chromatin Remodeler Required for Topoisomerase I Loading at Replication Forks. Cell Reports, 2016, 15 (2), pp.300-309. 10.1016/j.celrep.2016.03.027 . hal-02556384

HAL Id: hal-02556384

<https://hal.science/hal-02556384>

Submitted on 31 May 2021

HAL is a multi-disciplinary open access archive for the deposit and dissemination of scientific research documents, whether they are published or not. The documents may come from teaching and research institutions in France or abroad, or from public or private research centers.

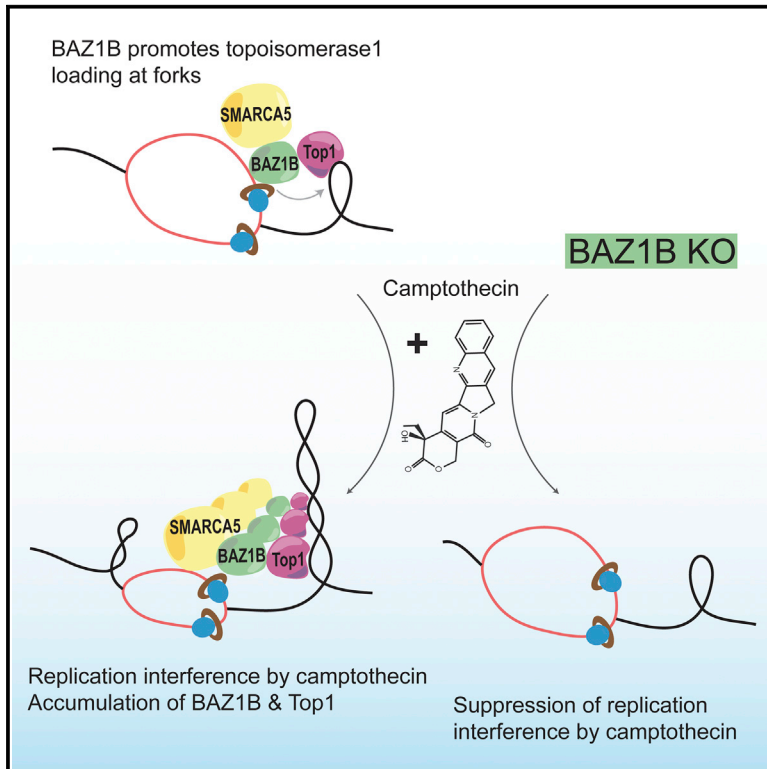
L'archive ouverte pluridisciplinaire **HAL**, est destinée au dépôt et à la diffusion de documents scientifiques de niveau recherche, publiés ou non, émanant des établissements d'enseignement et de recherche français ou étrangers, des laboratoires publics ou privés.



Distributed under a Creative Commons Attribution - NonCommercial - NoDerivatives 4.0 International License

Nascent DNA Proteomics Reveals a Chromatin Remodeler Required for Topoisomerase I Loading at Replication Forks

Graphical Abstract



Authors

Cyril Ribeyre, Ralph Zellweger, Maeva Chauvin, Nicole Bec, Christian Larroque, Massimo Lopes, Angelos Constantinou

Correspondence

cyril.ribeyre@igh.cnrs.fr (C.R.), angelos.constantinou@igh.cnrs.fr (A.C.)

In Brief

The topoisomerase I poison camptothecin exerts cytotoxicity against neoplastic cells through DNA replication interference. Ribeyre et al. identify proteins recruited at replication forks upon camptothecin exposure. They show that the chromatin remodeling complex BAZ1B-SMARCA5 promotes topoisomerase I loading near forks and determines the efficacy of replication interference by camptothecin.

Highlights

- Proteins are identified at replication forks upon treatment with camptothecin
- BAZ1B facilitates Top1 function during DNA replication
- The suppression of BAZ1B protects against camptothecin-induced fork interference



Nascent DNA Proteomics Reveals a Chromatin Remodeler Required for Topoisomerase I Loading at Replication Forks

Cyril Ribeyre,^{1,*} Ralph Zellweger,² Maeva Chauvin,¹ Nicole Bec,³ Christian Larroque,³ Massimo Lopes,² and Angelos Constantinou^{1,*}

¹Institute of Human Genetics, Centre National de la Recherche Scientifique (CNRS) UPR 1142, University of Montpellier, 34396 Montpellier, France

²Institute of Molecular Cancer Research, University of Zurich, 8057 Zurich, Switzerland

³Institut de Recherche en Cancérologie de Montpellier, INSERM, U1194, University of Montpellier, 34298 Montpellier, France

*Correspondence: cyril.ribeyre@igh.cnrs.fr (C.R.), angelos.constantinou@igh.cnrs.fr (A.C.)

<http://dx.doi.org/10.1016/j.celrep.2016.03.027>

SUMMARY

During transcription and DNA replication, the DNA template is overwound ahead of RNA and DNA polymerases and relaxed by DNA topoisomerases. Inhibitors of topoisomerases are potent anti-cancer agents. Camptothecin traps topoisomerase I on DNA and exerts preferential cytotoxicity toward cancer cells by way of its interference with the progression of replication forks. Starting with an unbiased proteomic analysis, we find that the chromatin remodeling complex BAZ1B-SMARCA5 accumulates near replication forks in camptothecin-exposed cells. We report that BAZ1B associates with topoisomerase I and facilitates its access to replication forks. Single-molecule analyses of replication structures show that BAZ1B contributes to replication interference by camptothecin. A lack of BAZ1B confers increased cellular tolerance of camptothecin. These findings reveal BAZ1B as a key facilitator of topoisomerase I function during DNA replication that affects the response of cancer cells to topoisomerase I inhibitors.

INTRODUCTION

Highly conserved DNA topoisomerases resolve DNA supercoils that build up during DNA replication and transcription (Pommier, 2006, 2013; Wang, 2002). Topoisomerase I (Top1) and topoisomerase II (Top2) preferentially localize to promoter regions of actively transcribed genes, where they promote gene expression together with chromatin-remodeling complexes (Durand-Dubief et al., 2010; Madabhushi et al., 2015; Puc et al., 2015; Sperling et al., 2011). In addition to their primary roles in transcription, Top1 and Top2 ensure the progression of replication forks and the maintenance of genome stability (Bermejo et al., 2007). Top1 notably prevents the formation of hybrid structures between nascent transcripts and their DNA template, called

R-loops, which obstruct the progress of replication forks (Sordet et al., 2009; Tuduri et al., 2009).

Topoisomerases are targeted by potent anti-cancer drugs (Pommier, 2006, 2013), and Top1 is the cellular target of the interfacial inhibitor camptothecin (CPT), a plant alkaloid that binds the interface of Top1-DNA cleavage complexes (Top1cc) and blocks Top1 cleavage/ligation cycles (Pommier, 2009). Although CPT is a powerful inhibitor of transcription, pioneering studies have shown that CPT cytotoxicity in proliferating cells results from interference between CPT-trapped Top1cc and moving DNA replication forks (Holm et al., 1989; Hsiang et al., 1989). CPT can induce replication-associated DNA double-strand breaks (DSBs) via replication runoff at Top1cc complexes (Strumberg et al., 2000). Whether or not replication-born DSBs account for the selective toxicity of CPT toward replicating cells is a matter of debate. Interfacial inhibitors of Top1 not only stabilize Top1cc but also prevent DNA uncoiling (Koster et al., 2007). So the mechanism of CPT-induced cell death during DNA replication may stem from the accumulation of DNA supercoils hindering the progression of replication forks. Consistent with this, low doses of CPT interfere with the progression of replication forks in the absence of detectable DSBs (Ray Chaudhuri et al., 2012). The direct visualization of replication intermediates by electron microscopy shows that CPT induces replication fork reversal into four-way junction, which protects against replication runoff at Top1cc (Ray Chaudhuri et al., 2012). Clearly, the mechanisms that determine the toxicity of CPT during DNA replication deserve further attention.

Here we examine how CPT interferes with the process of DNA replication. Using nascent DNA proteomics, we find a network of proteins that accumulates in the vicinity of the replication machinery within the first minutes of exposure to a mild dose of CPT. Among these proteins, we identify the chromatin-remodeling complex WICH, composed of BAZ1B and the ISWI ATPase SMARCA5. BAZ1B binds the DNA polymerase processivity factor PCNA and targets SMARCA5 to DNA replication factories, where it suppresses the formation of heterochromatin on newly synthesized DNA (Poot et al., 2004). We report here that BAZ1B promotes Top1 access to replication forks and, thereby, determines the efficacy of replication hindrance by CPT.

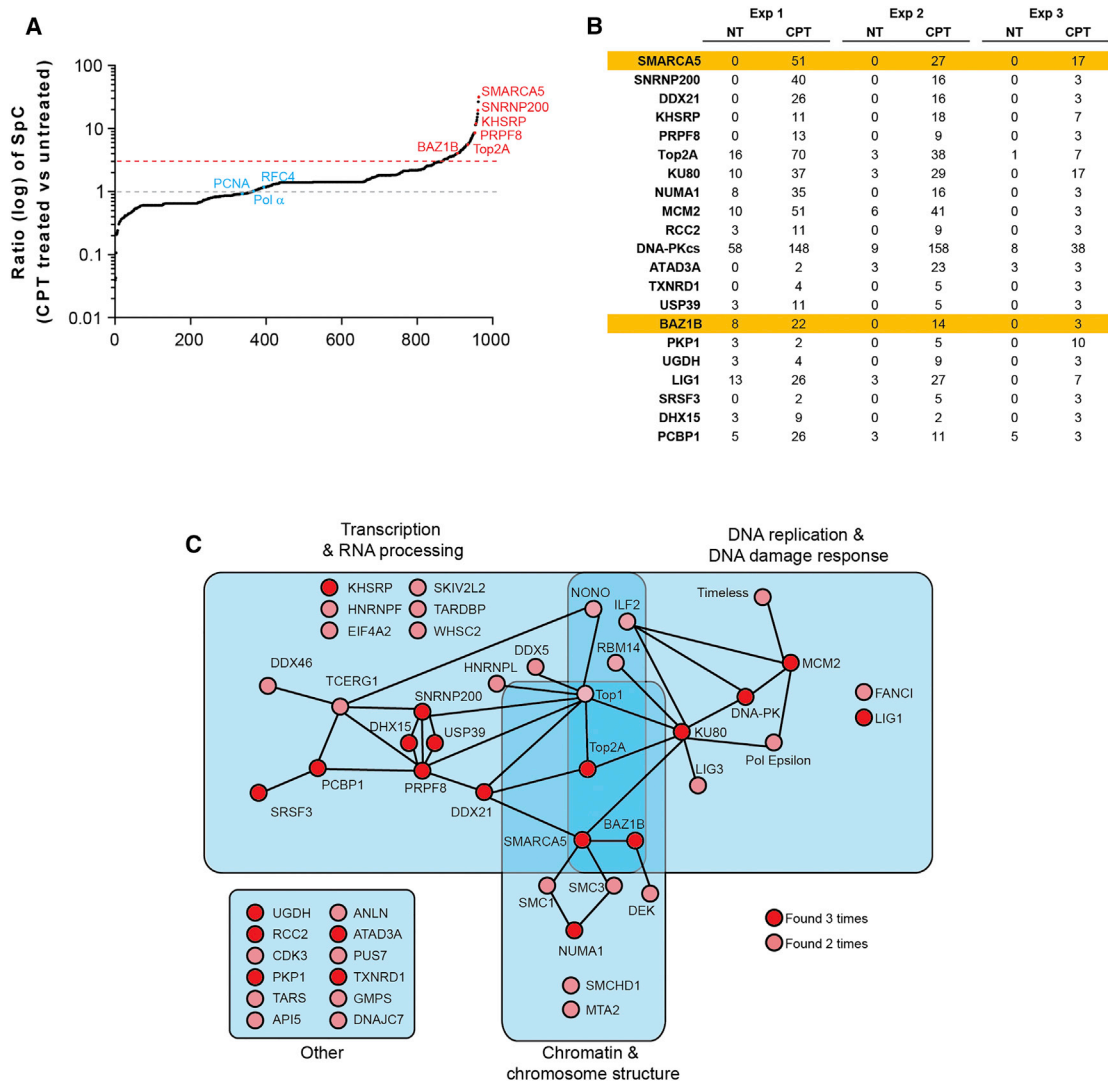


Figure 1. Proteins Enriched at CPT-Stalled Forks

(A) Proteins identified on nascent DNA are represented by the average ratio (three independent experiments) of normalized spectral counts (SpCs) detected in CPT-treated (this study) versus non-treated (NT) samples (Lossaint et al., 2013) and ranked in the order of increasing ratio. Each dot corresponds to one protein. (B) Table indicating the proteins enriched at least three times in average and detected in three independent experiments. The number of peptides detected by MS is shown. The entire set of data is available in Table S1.

(C) STRING network view of proteins enriched at CPT-stalled forks is shown (<http://string.embl.de>).

RESULTS

Systematic Identification of Protein Recruited at Replication Forks in the Presence of CPT

To identify molecular determinants of replication interference by Top1 inhibitors, we coupled the capture of isolation of proteins on nascent DNA with mass spectrometry (iPOND-MS) shortly after cell exposure to 100 nM CPT (Lossaint et al., 2013; Sirbu et al., 2011). Replication interference by CPT reduces the length of labeled replication tracks by ~50% (Ray Chaudhuri et al., 2012; Seiler et al., 2007). Thus, nascent DNA in untreated HeLa S3 was pulse-labeled with EdU for 5 min (Lossaint et al., 2013), while cells treated with 100 nM CPT were pulse-labeled for

10 min with EdU, in order to yield equivalent amounts of EdU-substituted DNA in untreated and CPT-treated cells. We purified proteins bound to EdU-labeled DNA, and we calculated the average ratio of normalized spectral counts for peptides identified by MS from three replicates of CPT-treated cells versus three replicates of untreated cells. The entire dataset is available in Table S1. Proteins were ranked in order of increasing ratios (Figure 1A).

We identified 21 proteins with a LogRatio ≥ 3 in three independent experiments (Figure 1B; Table S1). This group included the DNA repair and DNA replication proteins KU80, DNA-PKcs, MCM2, Top2A, and LIG1; the two components of the chromatin-remodeling complex WICH (BAZ1B and SMARCA5); the

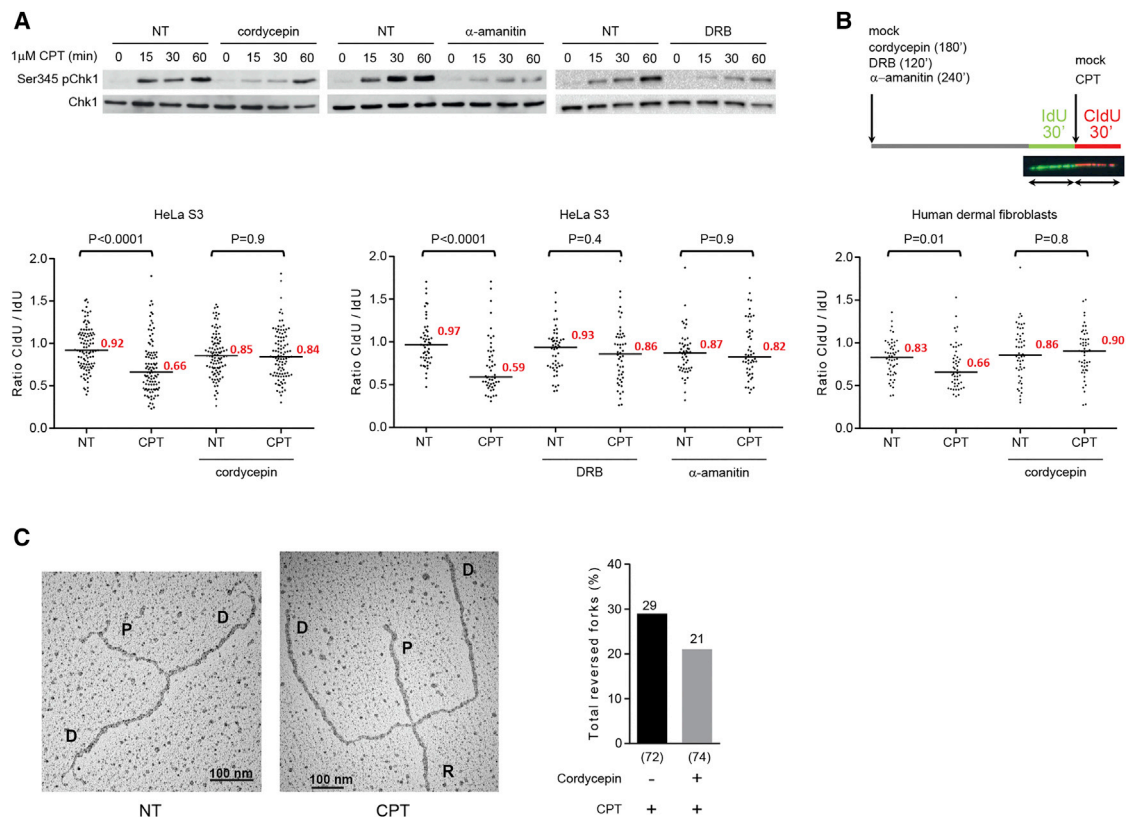


Figure 2. Transcription Is a Major Determinant of Replication Hindrance by CPT

(A) Western blot analysis of Chk1 phosphorylation on Ser345 in HeLa S3 cells exposed to CPT (1 μM) for the indicated time. When indicated, cells were pre-treated for 3 hr with 50 μM cordycepin, 4 hr with 50 μg/ml α-amanitin, or 2 hr with 100 μM DRB.

(B) HeLa S3 and HDF cells were pre-treated with transcription inhibitors as described above, and they were labeled with IdU (30 min) and then with CldU (30 min) in the presence of 1 μM CPT when indicated. Graphic representation shows the ratios of CldU versus IdU track length. The horizontal bar represents the median, indicated in red, from at least 50 replication tracks per experimental condition. Differences between experiments were assayed using Mann-Whitney rank test; p values are indicated.

(C) Frequency of reversed forks detected by electron microscopy (EM) in U2OS cells. Electron micrographs of a normal replication fork in non-treated cells and a regressed fork from CPT-treated cells are shown. Cells were treated for 1 hr with 25 nM CPT and pretreated or not for 3 hr with 50 μM cordycepin. The total number of analyzed molecules is given in brackets. Above each column, the percentage of reversed forks is indicated. Parental duplex, P; daughter duplex, D; regressed arm, R; NT, non-treated.

structural component of the nuclear matrix NUMA1; as well as proteins implicated in RNA metabolism (SNRNP200, KHSRP, PRPF8, USP39, DDX21, DHX15, SRSF3, and PCBP1). To obtain a broader perspective on the chromatin composition in the vicinity of replication forks upon inhibition of Top1, we also considered proteins that exhibited a LogRatio ≥ 4 in two of three independent experiments. This yielded a list of 50 proteins that form an interconnected functional network, as revealed by Search Tool for the Retrieval of Interacting Genes/Proteins (STRING) database analysis (Figure 1C).

Intriguingly, near half of the proteins enriched specifically at CPT-stalled forks were annotated as RNA-processing factors. Since transcription activity is a major source of DNA replication stress, we reasoned that the enrichment of RNA-processing factors near CPT-stalled forks could reflect proximity between transcription and DNA replication machineries. To verify the contribution of transcription activity on DNA replication interference by CPT (Liu and Wang, 1987), we transiently shut down

transcription with cordycepin, α-amanitin, or 5,6-dichloro-1-β-D-ribofurosylbenzimidazole (DRB). Transient inhibition of transcription did not alter the distribution of cells throughout the cell cycle (Figure S1A). We used Chk1 phosphorylation on Ser345 as a marker of CPT-induced DNA replication stress signaling. Phospho Chk1 (Ser345) signals were detected in HeLa S3 cells after 15-min exposure to CPT and accumulated thereafter (Figure 2A). By contrast, CPT-induced Chk1 phosphorylation was markedly reduced when the cells were pre-incubated with the transcription inhibitors cordycepin, α-amanitin, or DRB (Figure 2A).

Next we used DNA fiber labeling to measure the progression of replication forks in HeLa S3 cells and in primary human dermal fibroblasts (HDFs). Replication tracks were dually labeled with the thymidine analogs IdU and CldU for 30 min each (Merrick et al., 2004; Seiler et al., 2007). We did not observe significant differences in the length of IdU-labeled replication tracks synthesized in the absence or presence of cordycepin, α-amanitin, or

DRB (Figure S1B), indicating that transient inhibition of transcription activity per se did not perturb the progression of replication forks. Then we probed the impact of transcription activity on DNA replication interference by CPT. Under basal conditions, the ratios of CldU versus IdU track length was close to 1 (Figure 2B; Figure S1C), as expected if replisomes progress at constant speed. The addition of 1 μ M CPT during CldU pulse-labeling interfered with fork progression and reduced the length of CldU tracks. Hence, the ratio of CldU/IdU tracks was diminished. By contrast, replication interference by CPT was partially suppressed when transcription was inhibited by cordycepin, α -amanitin, or DRB (Figure 2B; Figure S1C). Next, we visualized replication intermediates using electron microscopy (Neelsen et al., 2014). Upon DNA replication stress, the nascent DNA strands can anneal and form a fourth arm extruded at the branch point, a process known as fork reversal (Ray Chaudhuri et al., 2012; Zellweger et al., 2015). Consistent with the notion that transcription stress contributes to DNA replication interference by CPT, the shutdown of transcription by cordycepin reduced the proportion of regressed forks in cells exposed to CPT (Figure 2C; Figure S1D). Altogether, these data indicate that CPT treatment exacerbates interference between transcription and DNA replication, thereby inducing accumulation of RNA-processing factors on nascent DNA near forks.

BAZ1B and SMARCA5 Accumulate at Replication Forks upon Top1 Inhibition

We sought to characterize specific factors actively recruited at replication forks that determine replication hindrance by CPT. MS analyses revealed a significant accumulation of BAZ1B and SMARCA5 proteins at CPT-stalled forks (Figure 1B). BAZ1B binds directly to the DNA polymerase processivity factor PCNA and targets the ISWI ATPase SMARCA5 to replication foci (Poot et al., 2004). The replication-dependent recruitment of this chromatin-remodeling complex on nascent DNA prompted us to examine the impact of BAZ1B function at replication forks during CPT treatment.

To validate iPOND-MS data, we repeated the iPOND and verified the binding of SMARCA5 and BAZ1B to nascent DNA by western blotting. Under basal conditions, weak signals corresponding to BAZ1B and SMARCA5 were detectable in pull-downs of EdU-labeled DNA, as reported previously (Lopez-Contreras et al., 2013; Sirbu et al., 2013). In the presence of CPT, however, the amount of SMARCA5 and BAZ1B bound to nascent DNA increased (Figure 3A). BAZ1B, SMARCA5, and PCNA signals were lost upon chase with thymidine, indicating that these proteins travel with replisomes (Figure 3A). When cells were treated with CPT for 10 min after thymidine chase, neither SMARCA5 nor BAZ1B was detected in EdU pull-downs that lacked PCNA (Figure 3B). This result confirms that CPT induces the accumulation of BAZ1B-SMARCA5 on nascent DNA specifically near replication forks (Figure 3B).

We generated a HeLa S3 cell line that stably expressed an anti-BAZ1B small hairpin RNA (shRNA). BAZ1B was efficiently depleted while the level of SMARCA5 remained unaffected (Figure 3C). In the absence of BAZ1B, we did not detect SMARCA5 on nascent DNA from CPT-treated cells (Figure 3D). Altogether, these data indicate that BAZ1B targets SMARCA5 on nascent

DNA and that both proteins accumulate near replication forks upon exposure to CPT.

BAZ1B-Depleted Cells Exhibit Increased Tolerance to CPT

Cells lacking BAZ1B (stable shRNA or knockout using CRISPR/Cas9) were viable, and their distribution into the cell cycle was not altered (Figure S2A), confirming that BAZ1B is not an essential factor (Culver-Cochran and Chadwick, 2013). BAZ1B loss of function, however, alters the profile of gene expression (Culver-Cochran and Chadwick, 2013; Lalli et al., 2016), consistent with the role of BAZ1B in chromatin remodeling. To confirm that the depletion of BAZ1B does not shut down transcription, we measured the rate of transcription activity using microscope quantification of nascent RNA transcripts labeled with the uridine analog EU (Adam et al., 2013). Figure 4A shows that, overall, the levels of transcription activity in BAZ1B-depleted and control cells are similar.

We analyzed the viability of BAZ1B-depleted cells following exposure to increasing concentrations of CPT for 3 days. BAZ1B-depleted cells were more tolerant to mild doses of CPT (125–500 nM) than control cells (Figure 4B). To confirm this result, we treated three independent *BAZ1B* knockout (KO) clones obtained by CRISPR/Cas9 with CPT. All three clones were more tolerant to CPT than controls cells, including two (clones 1 and 3) that were more tolerant to CPT than BAZ1B knockdown cells (Figure 4B). Importantly, the absence of BAZ1B did not alter the cellular level of Top1 (Figure S2B). Thus, increased tolerance to CPT was not caused by the downregulation of Top1. To confirm that BAZ1B suppression promotes cellular tolerance to CPT, we verified that CPT was still active in BAZ1B-depleted cells. Top1 is enriched in promoter regions of active genes (Durand-Dubief et al., 2010; Puc et al., 2015; Sperling et al., 2011), hence CPT primarily inhibits transcription. The incorporation of EU associated with transcription activity was decreased by 3-fold in both control and BAZ1B-depleted cells (Figure 4A), indicating that the absence of BAZ1B did not perturb the capacity of CPT to block transcription.

Next we examined if BAZ1B depletion increases tolerance to CPT via perturbation of DNA damage checkpoints. BAZ1B is endowed with a tyrosine kinase activity that contributes to the regulation of the late-stage DNA damage response via H2A.X phosphorylation on Tyr142 (Xiao et al., 2009). Consistent with this, we observed that the depletion of BAZ1B reduced the level of γ -H2AX by \sim 40% in HDFs exposed for 6 hr to 1 μ M CPT (Figure S2C). The depletion of BAZ1B did not induce constitutive phosphorylation of Chk1 on Ser345 and of RPA32 on Ser4/8 (Figure 4C), whereas both proteins were promptly phosphorylated upon cell exposure to CPT. The knockdown of BAZ1B with small interfering RNAs (siRNAs) slightly altered phospho-Chk1 (Ser345) and phospho-RPA32 (Ser4/8) signals in HDFs, but no clear difference in checkpoint signaling was observed in BAZ1B-depleted HeLa S3 cells (Figure 4C). This result confirms that BAZ1B depletion did not inhibit transcription-dependent phosphorylation of Chk1 in response to CPT treatment, as shown in Figure 2A. In summary, the depletion of BAZ1B promotes cellular tolerance to CPT without blocking transcriptional activity or inducing significant alterations in Chk1 phosphorylation.

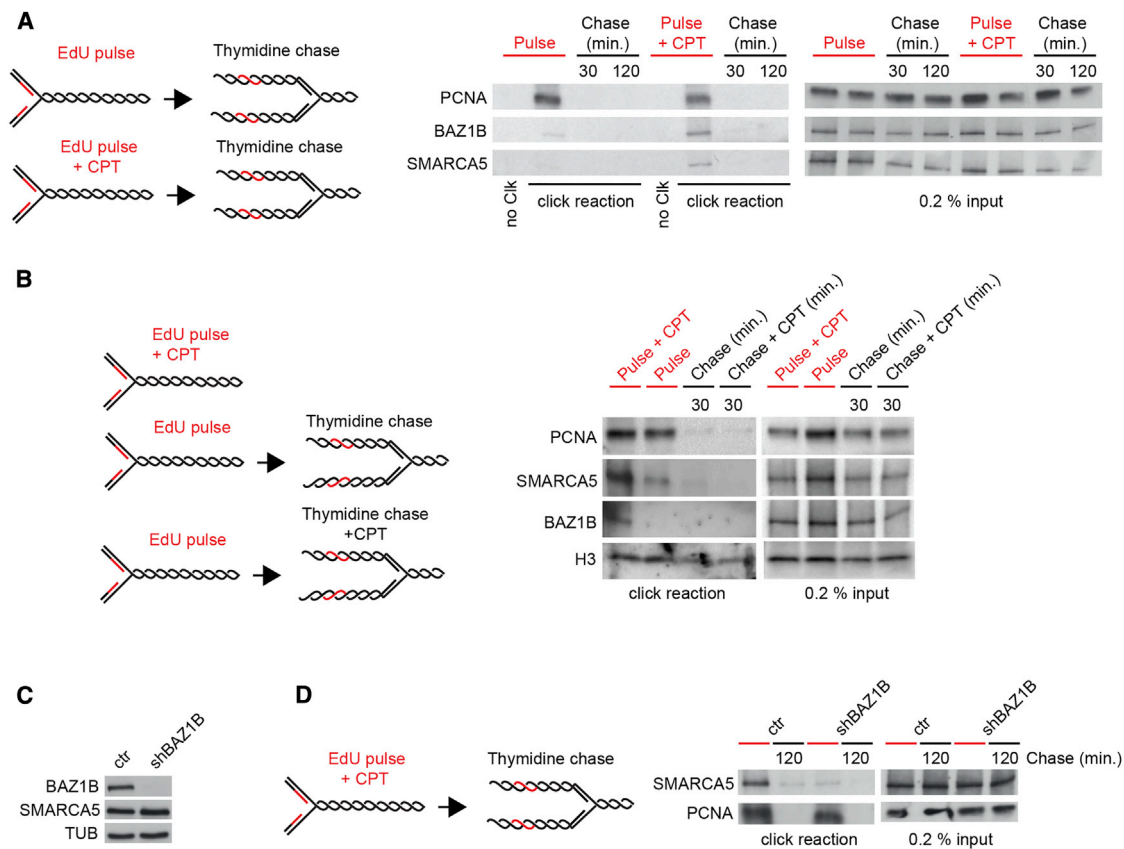


Figure 3. BAZ1B and SMARCA5 Accumulate on Nascent DNA upon CPT Treatment

(A) Western blot analysis of indicated proteins isolated by iPOND. HeLa S3 cells were pulse-labeled with EdU for 5 or 10 min in the presence of 1 μ M CPT, and then chased with thymidine for 30 or 120 min, as indicated. In no-click samples (no Clk), desthiobiotin-TEG azide was replaced by DMSO. (B) Western blot analysis of indicated proteins isolated by iPOND. HeLa S3 cells were pulse-labeled with EdU for 5 min under basal conditions or for 10 min in the presence of 1 μ M CPT, and then chased for 30 min with thymidine. When indicated, cells were exposed for 10 min to 1 μ M CPT after 30-min chase with thymidine. (C) Western blot analysis of the indicated proteins in HeLa S3 cells transfected with either pEB-H1-puro (Ctrl) or pEB-H1-puro shRNA BAZ1B is shown. (D) Control and BAZ1B-depleted HeLa S3 cells were pulse-labeled for 10 min with EdU in the presence of 1 μ M CPT, and then chased for 120 min with thymidine. The indicated proteins were isolated by iPOND and probed by western blotting.

BAZ1B Promotes Top1 Loading in the Vicinity of Replication Forks

Using iPOND, we detected Top1 on nascent DNA near replication forks (Figure 4D). This confirmed that, like in budding yeast (Bermejo et al., 2007), human Top1 associates with ongoing replication forks. The dynamic recruitment of Top1 on nascent DNA mirrored that of BAZ1B, and Top1 accumulated near replication forks upon exposure to CPT (Figure 4D), consistent with the iPOND-MS data (Table S1). Strikingly, the depletion of BAZ1B abolished the recruitment of Top1 to replication forks (Figure 4D). These data indicate that BAZ1B facilitates Top1 loading during DNA replication, but is dispensable for the function of Top1 in transcription.

We probed whether BAZ1B physically associates with Top1 by co-immunoprecipitation. Top1 was not detectable in immune precipitates of endogenous BAZ1B or in pull-downs of recombinant FLAG-BAZ1B expressed in HeLa S3 cells (data not shown). By contrast, we efficiently captured endogenous Top1 by immunoprecipitation, as revealed by Ponceau S staining of the nitrocellulose membrane after protein transfer (Figures 4E and 4F). Endogenous

BAZ1B co-immunoprecipitated with Top1, specifically. As expected, we did not detect BAZ1B in BAZ1B KO cells, confirming signal specificity (Figure 4E). The association of BAZ1B with Top1 was induced upon cell treatment with 1 μ M CPT for 30 min (Figure 4F). This association was unlikely to be mediated by bridging DNA molecules, as BAZ1B co-immunoprecipitated with Top1 in the presence of ethidium bromide (Figure 4F). Collectively, these data provide evidence that BAZ1B facilitates the recruitment of Top1 in the vicinity of replication forks.

BAZ1B Determines the Extent of CPT-Mediated Replication Fork Slowing and Reversal

Since BAZ1B promotes Top1 loading near forks, we examined if BAZ1B determines the capacity of CPT to hinder the progression of replication forks. We used DNA fiber labeling to monitor fork progression in HeLa S3 cells and in HDFs. Replication tracks were labeled using two consecutive 30-min pulses with IdU and CldU. The depletion of BAZ1B did not alter the average length of IdU tracks (Figure S3A), suggesting that, under these experimental conditions, BAZ1B does not influence the rate of

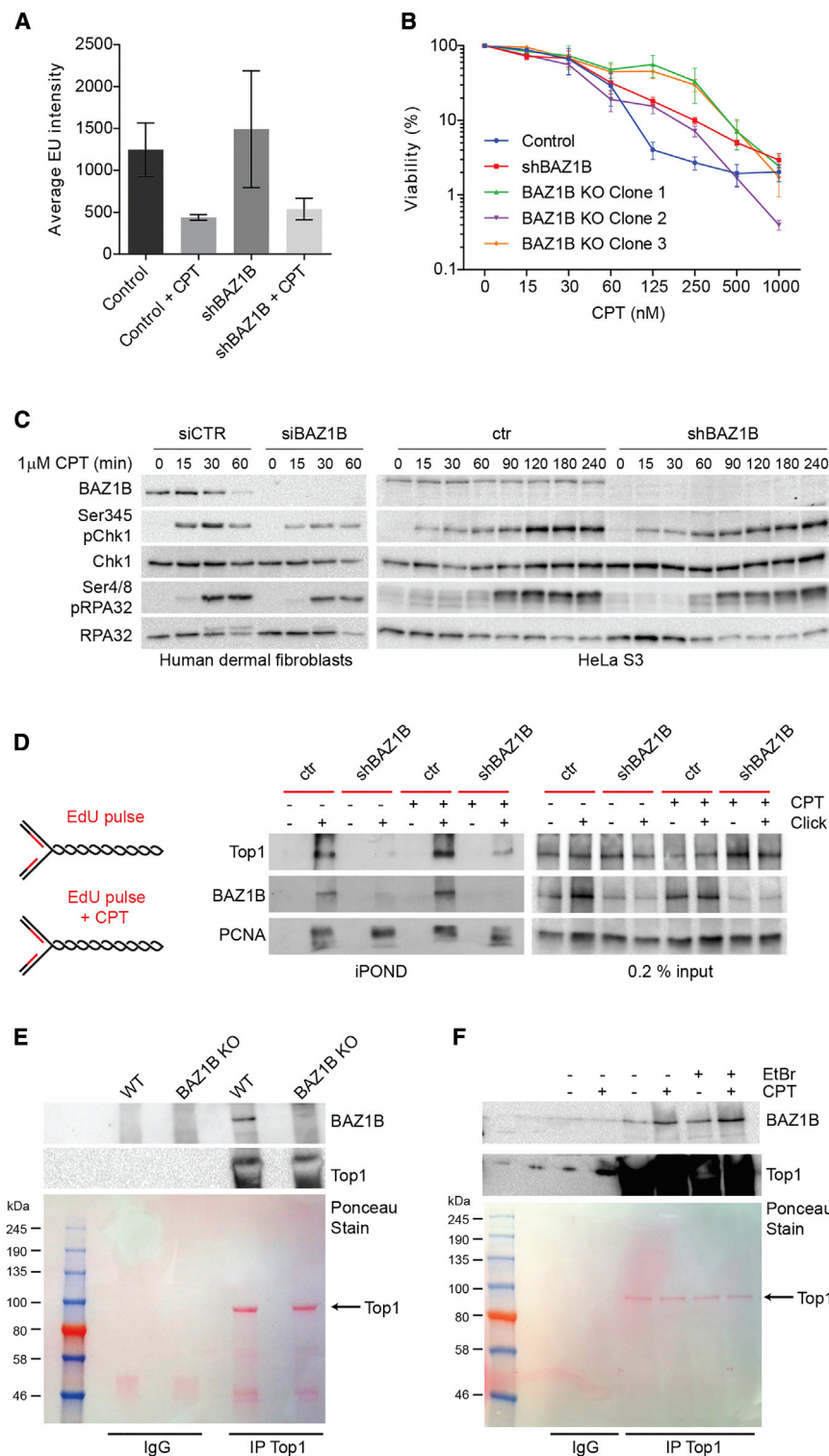


Figure 4. BAZ1B Promotes Top1 Loading in the Vicinity of Replication Forks

(A) Global transcriptional activity visualized by 5-ethynyl uridine (EU) incorporation. Cells were labeled with EU for 30 min with or without 1 μ M CPT. Average EU incorporation from three independent replicates was measured by fluorescence microscopy. At least 79 cells were analyzed per experiment. SD is indicated.

(B) Cells were treated with the indicated doses of CPT for 3 days. The percentage of viability was estimated using Promega CellTiter-Glo assay. The SEM from four independent experiments is indicated.

(C) HDFs transfected with control or anti-BAZ1B siRNA smartpool and HeLa S3 cells expressing an anti-BAZ1B shRNA were lysed after increasing exposure time in 1 μ M CPT, and then probed for the indicated proteins by western blotting. Total RPA32 signals fade away when RPA32 is phosphorylated, most likely owing to the dilution of the RPA32 signal into multiple bands corresponding to different degree of RPA32 phosphorylation.

(D) Western blot analysis of indicated proteins isolated on nascent DNA. Control and BAZ1B-depleted HeLa S3 cells were pulse-labeled with EdU for 5 or 10 min in the presence of 1 μ M CPT. (E) Western blot analysis of BAZ1B in Top1 immunoprecipitates from control and BAZ1B KO HeLa S3 cells, as indicated. The bottom panel shows the Ponceau staining of the nitrocellulose membrane after protein transfer. Top1 yields saturated ECL signals by western blotting.

(F) Western blot analysis of BAZ1B in Top1 immunoprecipitates from HeLa S3 cells treated with 1 μ M CPT for 30 min, and from extracts pretreated with 50 μ g/ml Ethidium Bromide (EtBr), as indicated. The Ponceau-stained nitrocellulose membrane is shown.

DNA chain elongation. In striking contrast, the knockdown of BAZ1B in HeLa S3 cells or in HDFs rescued fork progression in the presence of CPT, as revealed by the ratio of CldU/IdU tracks from cells exposed to CPT during CldU pulse-labeling (Figure 5A;

control cells, the percentage of regressed forks was reduced by \sim 30%, in BAZ1B knockdown and in BAZ1B KO cells (Figure 5E; Figure S4B), suggesting that BAZ1B activity at replication forks contributes to topological challenges induced by CPT. By

Figure S3B). Consistent with this, CPT did not hinder the progression of replication forks in three independent BAZ1B KO clones obtained by CRISPR/Cas9 (Figure 5B; Figure S4A). CPT-mediated replication interference was restored in BAZ1B KO cells complemented with *BAZ1B* cDNA (Figure 5C). Inhibition of DNA polymerase α by aphidicolin, however, interfered with DNA synthesis as efficiently in BAZ1B-depleted cells as in control cells, indicating that BAZ1B does not influence replication inhibition by a distinct mechanism (Figure 5D; Figure S5). Last, we used electron microscopy to score regressed forks in cells treated with CPT. In comparison with

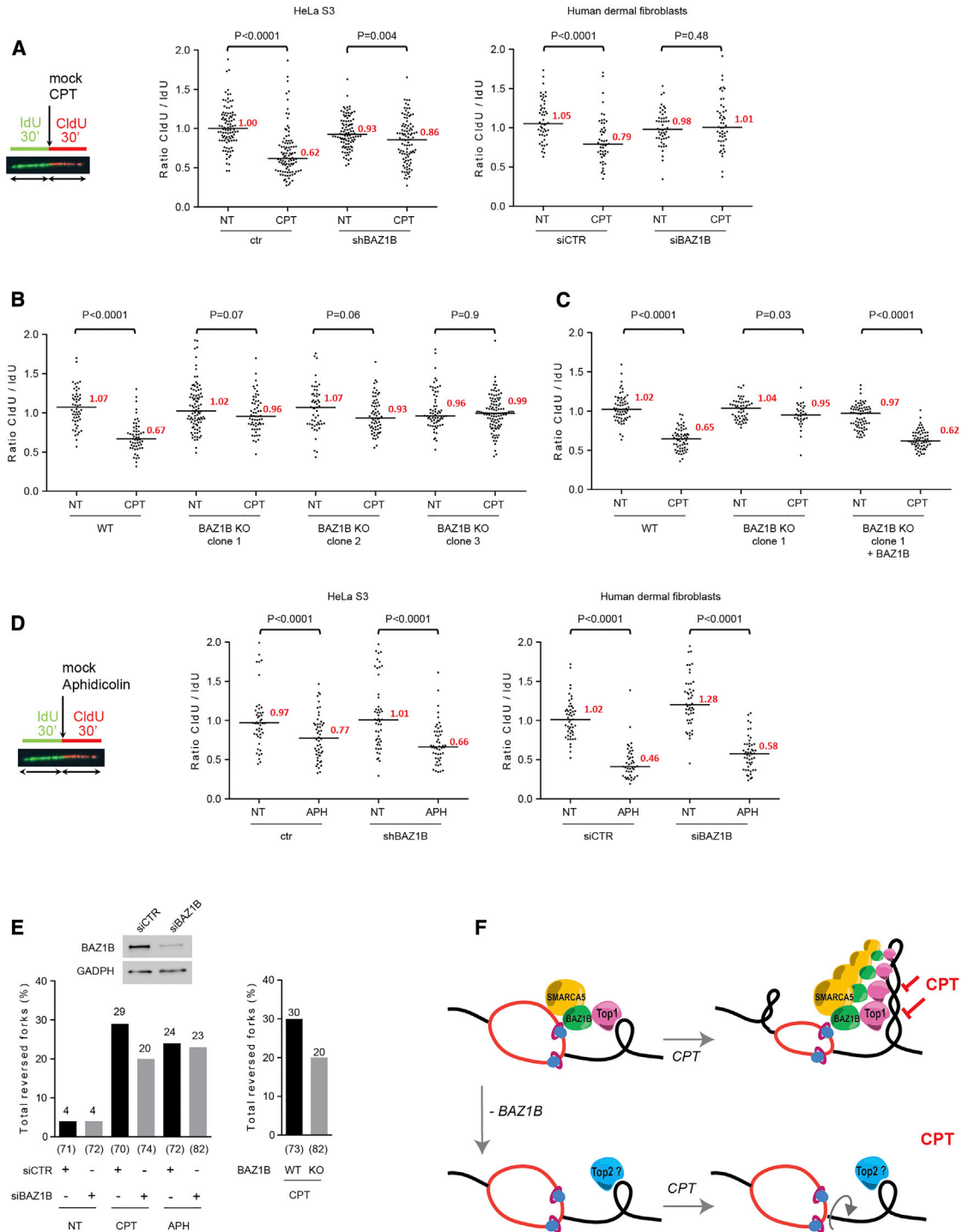


Figure 5. BAZ1B Determines Replication Interference and Fork Reversal by CPT

(A) HeLa S3 cells or HDFs were labeled with IdU (30 min) and then with CldU (30 min) in the presence of 1 μ M CPT, when indicated. Graphic representation shows the ratios of CldU versus IdU track length. The horizontal bar represents the median, indicated in red, from at least 50 replication tracks per experimental condition. Differences between experiments were assayed using Mann-Whitney rank test; p values are indicated.

(B) Replication tracks from HeLa S3 cells and three BAZ1B KO clones were prepared and analyzed as described in (A).

(C) Replication tracks from wild-type, BAZ1B KO, and BAZ1B KO HeLa S3 cells complemented with a cDNA encoding wild-type BAZ1B were prepared and analyzed as described in (A).

(legend continued on next page)

contrast, the frequency of regressed forks was similar in control and in BAZ1B knockdown cells exposed to aphidicolin (Figure 5E; Figure S4B). Collectively, these data indicate that BAZ1B specifically facilitates the function of Top1 and the action of CPT at replication forks.

DISCUSSION

Inhibitors of Top1 constitute an important class of chemotherapeutic drugs that exert cytotoxicity toward proliferating cancer cells via interference with ongoing replication forks (Holm et al., 1989; Hsiang et al., 1989). Our systematic analysis of proteins enriched near CPT-stalled forks revealed a network of transcription and pre-mRNA processing factors, suggesting that the topological constraints caused by CPT increase physical proximity between DNA replication and transcription machineries. Using transcription inhibitors, we show here that transcription activity contributes to replication interference by CPT, perhaps via the induction of hybrid structures between DNA and nascent transcripts, called R-loops, which represent major obstacles to the progression of replication forks (Sollier et al., 2014; Sordet et al., 2009; Zeman and Cimprich, 2014). Reactive aldehydes also interfere with DNA replication in a transcription-dependent manner via the induction of R-loops (Schwab et al., 2015). Free radicals, UV radiation, and alkylating drugs also can block the re-ligation of Top1cc and induce transcription stress (Meng et al., 2003; Pourquier and Pommier, 2001; Sordet et al., 2004). These agents generate chemical alterations in DNA that perturb the perfect alignment of the 5' hydroxyl end and the tyrosyl-phosphodiester bonds necessary to re-ligate Top1cc complexes. Thus, as shown here for CPT, replication interference by DNA-damaging agents that perturb Top1 cleavage/ligation cycles could be associated with the induction of conflicts between transcription and DNA replication.

In this study, we report the identification of the replication-associated chromatin-remodeling complex WICH (BAZ1B-SMARCA5) as a key determinant of replication hindrance by Top1 poisons. We do not believe that the contribution of BAZ1B in replication hindrance by CPT is linked with an essential function of BAZ1B in transcription. The depletion of BAZ1B did not shut down transcription, did not perturb the capacity of CPT to block transcription, and did not inhibit transcription-dependent Chk1 phosphorylation upon treatment with CPT. Cells lacking BAZ1B grow like normal cells and the KO of *BAZ1B* is compatible with human life. BAZ1B is deleted along with ~26–28 genes on chromosome 7q11.23 in a neurodevelopmental disorder known as Williams-Beuren syndrome (Francke, 1999), a condition characterized by developmental delay, cardiovascular anomalies, and abnormal social-emotional processing.

We present evidence that BAZ1B promotes Top1 function during DNA replication. First, BAZ1B was necessary for Top1

binding at replication forks, and both proteins accumulated on nascent DNA upon Top1 inhibition; second, endogenous Top1 and BAZ1B co-immunoprecipitated in a CPT-inducible manner; last, BAZ1B determined replication interference and fork reversal by CPT. As Top1 inhibitors prevent DNA uncoiling by Top1 (Koster et al., 2007), the accumulation of positive supercoiling ahead of replication forks can be absorbed by fork reversal (Postow et al., 2001). Consistent with BAZ1B promoting Top1 function near replication forks, the depletion of BAZ1B partially suppressed the reversal of replication forks.

BAZ1B is recruited to replication factories through direct interaction with PCNA (Poot et al., 2004, 2005). We propose that BAZ1B recruitment at forks promotes Top1 action and thereby counteracts the accumulation of positive supercoiling ahead of the advancing replication machine (Figure 5F). The depletion of BAZ1B did not induce replication defects or replication stress signaling under basal conditions, suggesting that the loading of Top1 by BAZ1B at replication forks is not essential for DNA replication. The accumulation of supercoiled DNA during replication may be resolved via other mechanisms. For example, if replication forks are free to swivel around their axis, torsional stress ahead of replication forks can redistribute to the replicated sister duplexes as pre-catenanes resolved by type II topoisomerases.

The chromatin-remodeling complex BAZ1B-SMARCA5 may respond to the accumulation of DNA supercoiling at replication forks via the detection of alterations in nucleosome positioning caused by topological stress. Naked supercoiled DNA is efficiently processed by topoisomerases, but nucleosomes represent an obstacle to the resolution of supercoils (Halmer and Gruss, 1997). As CPT perturbs nucleosome turnover (Teves and Henikoff, 2014), BAZ1B-SMARCA5 (WICH complex) may facilitate Top1 accessibility to the vicinity of replication forks via nucleosome remodeling. A non-mutually exclusive possibility is that the remodeling of nucleosomes by BAZ1B-SMARCA5 near forks induces the accumulation of DNA supercoiling resolved by Top1 (Gavin et al., 2001). The functional association between chromatin remodeling and DNA uncoiling is not without precedent. For example, BRG1/SMARCA4 and BAF250a/ARID1A from the SWI/SNF BAF complex recruit topoisomerase IIA to chromatin (Dykhuizen et al., 2013). Likewise, Top2 recruitment in budding yeast depends on Snf5, a component of the SWI/SNF complex (Sperling et al., 2011). Very recently, BRG1/SMARCA4 and the FACT complex have been shown to be required for Top1 recruitment at immunoglobulin loci (Husain et al., 2016).

The non-essential function of BAZ1B in Top1 loading near replications forks suggests in principle BAZ1B as a candidate biomarker to guide the rational use of Top1 inhibitors. As the anti-cancer property of Top1 inhibitors is linked with DNA replication hindrance, measurements of BAZ1B levels in tumor tissues could help predict therapeutic outcomes.

(D) HeLa S3 cells or HDFs were labeled with IdU (30 min) and then with CldU (30 min) in the presence of aphidicolin (0.1 μ M), as indicated. Ratios of CldU/IdU track length were analyzed as described in (A).

(E) Frequency of reversed forks detected by EM in BAZ1B knockdown U2OS cells and in BAZ1B KO HeLa S3 cells, as indicated. The knockdown of BAZ1B was verified by western blotting. GAPDH was used as a loading control. Cells were optionally treated for 1 hr with 25 nM CPT or 0.1 μ M aphidicolin. The number of molecules analyzed is given in brackets. The percentage of reversed forks is indicated. Similar results were obtained in at least one independent experiment.

(F) Model: BAZ1B facilitates Top1 loading near replication forks and determines the efficacy of replication interference by CPT.

EXPERIMENTAL PROCEDURES

Cell Lines

HDFs from neonatal human foreskin were maintained in DMEM plus 10% fetal calf serum (FCS) and L-glutamine (2 mM). HeLa S3 and human osteosarcoma U2OS were maintained in DMEM plus 10% FCS and penicillin-streptomycin (1%).

shRNA and siRNA

The shRNA against BAZ1B (5'-GGAGATAGTTCGATACTTTAT-3') was cloned in pEB-H1-puro (a gift from Joachim Lingner) and used to generate the stable HeLa S3 cell line using lipofectamine (Life Technologies) for transfection. SmartPool BAZ1B siRNA (M-006901-02-005) and control siRNA (M-001810-02-005) were from Dharmacon. Analyses were performed 48 hr after transfection.

CRISPR/Cas9

The two RNA guides (sequences available on request) for targeting BAZ1B exon 2 were designed using the CRISPR design website (<http://crispr.mit.edu/>) and cloned in MLM3636. The two plasmids were then co-transfected with pHL-EF1a-SphcCas9(D10A)-iP-A that encodes the Cas9 nickase. Individual clones were tested for BAZ1B expression by western blotting. Complementation was performed using pEBAZ1B (a gift from P. Varga-Weisz), which encodes BAZ1B under the control of CMV promoter.

MS and Label-free Quantification

Matrix-assisted laser desorption/ionization tandem MS (MS/MS) analyses and label-free quantification were performed as described previously (Lossaint et al., 2013).

iPOND

iPOND was performed as described in Lossaint et al. (2013) and in the Supplemental Experimental Procedures.

Western Blotting

Samples were resolved by SDS-PAGE and transferred on nitrocellulose membranes. Antibodies against the following proteins were used: BAZ1B (Bethyl Laboratories, A300-446A), SMARCA5 (Bethyl Laboratories, A301-017A), Ser345 Phospho-Chk1 (Cell Signaling Technology, 2348), Chk1 (Santa Cruz Biotechnology, sc-8408), PCNA (Sigma-Aldrich, P8825), H3 (Santa Cruz Biotechnology, sc-10809) Tubulin (GeneTex, GTX27749), Ser4/8 Phospho RPA32 (Bethyl Laboratories, A300-245A), RPA32 (Calbiochem, NA18), and Top1 (BD Pharmingen, 556597).

DNA Fiber Labeling

DNA fiber labeling was performed as described in Lossaint et al. (2013) and in the Supplemental Experimental Procedures. Differences between experiments were assayed using the Mann-Whitney rank test.

EU Incorporation

HeLa S3 cells were incubated for 30 min with 5-ethynyl uridine (EU) and fixed with 4% paraformaldehyde. EU was coupled with Alexa fluor 555 with a Click-IT kit (Life Technologies). Cells were analyzed by fluorescence microscopy and average EU intensity was calculated using ImageJ software.

Survival and Viability

HeLa S3 cells were incubated with increasing concentrations of CPT for 3 days and viability was estimated using CellTiter-GLO (Promega).

Electron Microscopy Analysis of DNA Replication Intermediates in Human Cells

The procedure was essentially performed as described in Neelsen et al. (2014) and in the Supplemental Experimental Procedures.

Co-immunoprecipitation

HeLa cells were incubated for 30 min on ice in high-salt buffer (50 mM Tris [pH 7.5], 300 mM NaCl, 1% Triton, and 1 mM DTT). After 10-min centrifugation

at 14,000 × g, supernatant was incubated with anti-Top1 antibody (Abcam, ab109374) or IgG rabbit (Calbiochem, NI01) overnight at 4°C. Magnetic beads coupled with protein G (Life Technologies, 10004D) were added for 1 hr and washed five times with washing buffer (10 mM HEPES, 100 mM KOAc, and 0.1 mM MgOAc). Beads were boiled in Laemmli buffer and supernatants were analyzed by western blotting.

SUPPLEMENTAL INFORMATION

Supplemental Information includes Supplemental Experimental Procedures, five figures, and one table and can be found with this article online at <http://dx.doi.org/10.1016/j.celrep.2016.03.027>.

AUTHOR CONTRIBUTIONS

Conceptualization, C.R. and A.C.; Methodology and Investigation, C.R. and M.C.; Electron Microscopy, R.Z. and M.L.; Mass Spectrometry, N.B. and C.L.; Writing, C.R. and A.C.

ACKNOWLEDGMENTS

We thank Patrick Varga-Weisz, Vjekoslav Dulic, and Gérald Lossaint for reagents; Philippe Pasero and the laboratory members for comments on the manuscript; and Philippe Pourquier for advice. This work was supported by grants from the Fondation ARC pour la Recherche sur le Cancer, the Agence Nationale pour la Recherche, and la Fondation de France (to A.C.), La Ligue contre le Cancer Hérault and Projet Fondation ARC (to C.R.), and a European Research Council Consolidator (to M.L.).

Received: August 6, 2015

Revised: February 18, 2016

Accepted: March 6, 2016

Published: March 31, 2016

REFERENCES

- Adam, S., Polo, S.E., and Almouzni, G. (2013). Transcription recovery after DNA damage requires chromatin priming by the H3.3 histone chaperone HIRA. *Cell* 155, 94–106.
- Bermejo, R., Doksan, Y., Capra, T., Katou, Y.M., Tanaka, H., Shirahige, K., and Foiani, M. (2007). Top1- and Top2-mediated topological transitions at replication forks ensure fork progression and stability and prevent DNA damage checkpoint activation. *Genes Dev.* 21, 1921–1936.
- Culver-Cochran, A.E., and Chadwick, B.P. (2013). Loss of WSTF results in spontaneous fluctuations of heterochromatin formation and resolution, combined with substantial changes to gene expression. *BMC Genomics* 14, 740.
- Durand-Dubief, M., Persson, J., Norman, U., Hartsuiker, E., and Ekwall, K. (2010). Topoisomerase I regulates open chromatin and controls gene expression in vivo. *EMBO J.* 29, 2126–2134.
- Dykhuizen, E.C., Hargreaves, D.C., Miller, E.L., Cui, K., Korshunov, A., Kool, M., Pfister, S., Cho, Y.J., Zhao, K., and Crabtree, G.R. (2013). BAF complexes facilitate decatenation of DNA by topoisomerase II α . *Nature* 497, 624–627.
- Francke, U. (1999). Williams-Beuren syndrome: genes and mechanisms. *Hum. Mol. Genet.* 8, 1947–1954.
- Gavin, I., Horn, P.J., and Peterson, C.L. (2001). SWI/SNF chromatin remodeling requires changes in DNA topology. *Mol. Cell* 7, 97–104.
- Halmer, L., and Gruss, C. (1997). Accessibility to topoisomerases I and II regulates the replication efficiency of simian virus 40 minichromosomes. *Mol. Cell. Biol.* 17, 2624–2630.
- Holm, C., Covey, J.M., Kerrigan, D., and Pommier, Y. (1989). Differential requirement of DNA replication for the cytotoxicity of DNA topoisomerase I and II inhibitors in Chinese hamster DC3F cells. *Cancer Res.* 49, 6365–6368.
- Hsiang, Y.H., Liu, L.F., Wall, M.E., Wani, M.C., Nicholas, A.W., Manikumar, G., Kirschenbaum, S., Silber, R., and Potmesil, M. (1989). DNA topoisomerase

- I-mediated DNA cleavage and cytotoxicity of camptothecin analogues. *Cancer Res.* **49**, 4385–4389.
- Husain, A., Begum, N.A., Taniguchi, T., Taniguchi, H., Kobayashi, M., and Honjo, T. (2016). Chromatin remodeler SMARCA4 recruits topoisomerase I and suppresses transcription-associated genomic instability. *Nat. Commun.* **7**, 10549.
- Koster, D.A., Palle, K., Bot, E.S., Bjornsti, M.A., and Dekker, N.H. (2007). Antitumour drugs impede DNA uncoiling by topoisomerase I. *Nature* **448**, 213–217.
- Lalli, M.A., Jang, J., Park, J.C., Wang, Y., Guzman, E., Zhou, H., Audouard, M., Bridges, D., Tovar, K.R., Papuc, S.M., et al. (2016). Haploinsufficiency of BAZ1B contributes to Williams syndrome through transcriptional dysregulation of neurodevelopmental pathways. *Hum. Mol. Genet.*, ddw010.
- Liu, L.F., and Wang, J.C. (1987). Supercoiling of the DNA template during transcription. *Proc. Natl. Acad. Sci. USA* **84**, 7024–7027.
- Lopez-Contreras, A.J., Ruppen, I., Nieto-Soler, M., Murga, M., Rodriguez-Acebes, S., Remeseiro, S., Rodrigo-Perez, S., Rojas, A.M., Mendez, J., Muñoz, J., and Fernandez-Capetillo, O. (2013). A proteomic characterization of factors enriched at nascent DNA molecules. *Cell Rep.* **3**, 1105–1116.
- Lossaint, G., Larroque, M., Ribeyre, C., Bec, N., Larroque, C., Décaillet, C., Gari, K., and Constantinou, A. (2013). FANCD2 binds MCM proteins and controls replisome function upon activation of S phase checkpoint signaling. *Mol. Cell* **51**, 678–690.
- Madabhushi, R., Gao, F., Pfenning, A.R., Pan, L., Yamakawa, S., Seo, J., Rueda, R., Phan, T.X., Yamakawa, H., Pao, P.C., et al. (2015). Activity-Induced DNA Breaks Govern the Expression of Neuronal Early-Response Genes. *Cell* **161**, 1592–1605.
- Meng, L.H., Liao, Z.Y., and Pommier, Y. (2003). Non-camptothecin DNA topoisomerase I inhibitors in cancer therapy. *Curr. Top. Med. Chem.* **3**, 305–320.
- Merrick, C.J., Jackson, D., and Diffley, J.F. (2004). Visualization of altered replication dynamics after DNA damage in human cells. *J. Biol. Chem.* **279**, 20067–20075.
- Neelsen, K.J., Chaudhuri, A.R., Follonier, C., Herrador, R., and Lopes, M. (2014). Visualization and interpretation of eukaryotic DNA replication intermediates in vivo by electron microscopy. *Methods Mol. Biol.* **1094**, 177–208.
- Pommier, Y. (2006). Topoisomerase I inhibitors: camptothecins and beyond. *Nat. Rev. Cancer* **6**, 789–802.
- Pommier, Y. (2009). DNA topoisomerase I inhibitors: chemistry, biology, and interfacial inhibition. *Chem. Rev.* **109**, 2894–2902.
- Pommier, Y. (2013). Drugging topoisomerases: lessons and challenges. *ACS Chem. Biol.* **8**, 82–95.
- Poot, R.A., Bozhenok, L., van den Berg, D.L., Steffensen, S., Ferreira, F., Grimaldi, M., Gilbert, N., Ferreira, J., and Varga-Weisz, P.D. (2004). The Williams syndrome transcription factor interacts with PCNA to target chromatin remodeling by ISWI to replication foci. *Nat. Cell Biol.* **6**, 1236–1244.
- Poot, R.A., Bozhenok, L., van den Berg, D.L., Hawkes, N., and Varga-Weisz, P.D. (2005). Chromatin remodeling by WSTF-ISWI at the replication site: opening a window of opportunity for epigenetic inheritance? *Cell Cycle* **4**, 543–546.
- Postow, L., Crisona, N.J., Peter, B.J., Hardy, C.D., and Cozzarelli, N.R. (2001). Topological challenges to DNA replication: conformations at the fork. *Proc. Natl. Acad. Sci. USA* **98**, 8219–8226.
- Pourquier, P., and Pommier, Y. (2001). Topoisomerase I-mediated DNA damage. *Adv. Cancer Res.* **80**, 189–216.
- Puc, J., Kozbial, P., Li, W., Tan, Y., Liu, Z., Suter, T., Ohgi, K.A., Zhang, J., Aggarwal, A.K., and Rosenfeld, M.G. (2015). Ligand-dependent enhancer activation regulated by topoisomerase-I activity. *Cell* **160**, 367–380.
- Ray Chaudhuri, A., Hashimoto, Y., Herrador, R., Neelsen, K.J., Fachinetti, D., Bermejo, R., Cocito, A., Costanzo, V., and Lopes, M. (2012). Topoisomerase I poisoning results in PARP-mediated replication fork reversal. *Nat. Struct. Mol. Biol.* **19**, 417–423.
- Schwab, R.A., Nieminuszczy, J., Shah, F., Langton, J., Lopez Martinez, D., Liang, C.C., Cohn, M.A., Gibbons, R.J., Deans, A.J., and Niedzwiedz, W. (2015). The Fanconi Anemia Pathway Maintains Genome Stability by Coordinating Replication and Transcription. *Mol. Cell* **60**, 351–361.
- Seiler, J.A., Conti, C., Syed, A., Aladjem, M.I., and Pommier, Y. (2007). The intra-S-phase checkpoint affects both DNA replication initiation and elongation: single-cell and -DNA fiber analyses. *Mol. Cell Biol.* **27**, 5806–5818.
- Sirbu, B.M., Couch, F.B., Feigler, J.T., Bhaskara, S., Hiebert, S.W., and Cortez, D. (2011). Analysis of protein dynamics at active, stalled, and collapsed replication forks. *Genes Dev.* **25**, 1320–1327.
- Sirbu, B.M., McDonald, W.H., Dungalwala, H., Badu-Nkansah, A., Kavanaugh, G.M., Chen, Y., Tabb, D.L., and Cortez, D. (2013). Identification of proteins at active, stalled, and collapsed replication forks using isolation of proteins on nascent DNA (iPOND) coupled with mass spectrometry. *J. Biol. Chem.* **288**, 31458–31467.
- Sollier, J., Stork, C.T., Garcia-Rubio, M.L., Paulsen, R.D., Aguilera, A., and Cimprich, K.A. (2014). Transcription-coupled nucleotide excision repair factors promote R-loop-induced genome instability. *Mol. Cell* **56**, 777–785.
- Sordet, O., Liao, Z., Liu, H., Antony, S., Stevens, E.V., Kohlhagen, G., Fu, H., and Pommier, Y. (2004). Topoisomerase I-DNA complexes contribute to arsenic trioxide-induced apoptosis. *J. Biol. Chem.* **279**, 33968–33975.
- Sordet, O., Redon, C.E., Guirouilh-Barbat, J., Smith, S., Solier, S., Douarre, C., Conti, C., Nakamura, A.J., Das, B.B., Nicolas, E., et al. (2009). Ataxia telangiectasia mutated activation by transcription- and topoisomerase I-induced DNA double-strand breaks. *EMBO Rep.* **10**, 887–893.
- Sperling, A.S., Jeong, K.S., Kitada, T., and Grunstein, M. (2011). Topoisomerase II binds nucleosome-free DNA and acts redundantly with topoisomerase I to enhance recruitment of RNA Pol II in budding yeast. *Proc. Natl. Acad. Sci. USA* **108**, 12693–12698.
- Strumberg, D., Pilon, A.A., Smith, M., Hickey, R., Malkas, L., and Pommier, Y. (2000). Conversion of topoisomerase I cleavage complexes on the leading strand of ribosomal DNA into 5'-phosphorylated DNA double-strand breaks by replication runoff. *Mol. Cell Biol.* **20**, 3977–3987.
- Teves, S.S., and Henikoff, S. (2014). Transcription-generated torsional stress destabilizes nucleosomes. *Nat. Struct. Mol. Biol.* **21**, 88–94.
- Tuduri, S., Crabbé, L., Conti, C., Tourrière, H., Holtgreve-Grez, H., Jauch, A., Pantescio, V., De Vos, J., Thomas, A., Theillet, C., et al. (2009). Topoisomerase I suppresses genomic instability by preventing interference between replication and transcription. *Nat. Cell Biol.* **11**, 1315–1324.
- Wang, J.C. (2002). Cellular roles of DNA topoisomerases: a molecular perspective. *Nat. Rev. Mol. Cell Biol.* **3**, 430–440.
- Xiao, A., Li, H., Shechter, D., Ahn, S.H., Fabrizio, L.A., Erdjument-Bromage, H., Ishibe-Murakami, S., Wang, B., Tempst, P., Hofmann, K., et al. (2009). WSTF regulates the H2A.X DNA damage response via a novel tyrosine kinase activity. *Nature* **457**, 57–62.
- Zellweger, R., Dalcher, D., Mutreja, K., Berti, M., Schmid, J.A., Herrador, R., Vindigni, A., and Lopes, M. (2015). Rad51-mediated replication fork reversal is a global response to genotoxic treatments in human cells. *J. Cell Biol.* **208**, 563–579.
- Zeman, M.K., and Cimprich, K.A. (2014). Causes and consequences of replication stress. *Nat. Cell Biol.* **16**, 2–9.